Hindawi
Journal of Nanomaterials
Volume 2019, Article ID 7962754, 9 pages
https://doi.org/10.1155/2019/7962754

Research Article

Preparation and Conductive and Electromagnetic Properties of Fe_3O_4/PANI Nanocomposite via Reverse In Situ Polymerization

Di Zhang, Huaiyin Chen, and Ruoyu Hong

College of Chemical Engineering, Fuzhou University, Fuzhou, Fujian 350108, China

Correspondence should be addressed to Ruoyu Hong; rhong@fzu.edu.cn

Di Zhang and Huaiyin Chen contributed equally to this work.

Received 30 September 2019; Revised 7 November 2019; Accepted 16 November 2019; Published 5 December 2019

Academic Editor: You Qiang

In this paper, the magnetite/polyaniline (PANI) nanocomposite was prepared by the novel reverse in situ polymerization method. Fe_3O_4 magnetic nanoparticles were synthesized in situ in PANI chloroform solution to form a suspension containing the Fe_3O_4/PANI nanocomposite. It overcame the disadvantage of oxidation of the Fe_3O_4 by the oxidant in conventional method. The Fe_3O_4/PANI chloroform suspension and the Fe_3O_4/PANI powder were characterized by FT-IR, TEM, XRD, vibrating sample magnetometer, Gouy magnetic balance, conductivity meter, and vector network analyzer. It is demonstrated that the Fe_3O_4/PANI suspension has a good electrical conductivity that is up to 2.135 μS/cm at the optimal ratio of reactants. The Fe_3O_4 nanoparticles are well dispersed in the PANI network with a particle size of about 10 nm. Fe_3O_4/PANI powder has high saturation magnetization and magnetic susceptibility, as well as a broad application prospect in the field of electromagnetic devices. The Fe_3O_4/PANI powder exhibits an excellent microwave absorption behavior, which can be an outstanding candidate for the rapid development of broadband shielding materials.

1. Introduction

In recent years, with the development of science and technology, more and more wireless devices have appeared in human society. These wireless systems bring convenience to people's lives, but in the meantime show many negative effects. Firstly, the human body will suffer a series of diseases under the electromagnetic radiation with high intensity for a long time. Secondly, the surrounding electromagnetic waves will cause Electromagnetic Interference (EMI). It is of great significance to develop efficient absorbing materials to solve the electromagnetic pollution [1–4].

While searching for more effective absorbing agents, people are paying increasing attention to the nanocomposite of magnetic particle and conductive polymer. Some previously reported studies have shown that the magnetic conductive polymers have a high spin density and exhibit ferromagnetic and antiferromagnetic properties, which have broad application prospects in sensing technology, nonlinear optical materials, molecular electrical devices, medical research, electromagnetic shielding, and microwave absorption [5–9].

The magnetic particle-conductive polymer nanocomposite generally possesses the core-shell structures. Most of them are composed of metal oxides (such as iron, cobalt, nickel, and other oxides) as the core and polymer materials as the shell, while a small part is made of a polymeric material as a core and an inorganic magnetic material as a shell layer. In addition, there exists a sandwich structure, with the outer and inner interlayers of polymeric materials and the middle interlayer of inorganic particles [10–12]. In general, the core-shell materials have special conductivity, magnetic properties, and microwave absorption properties due to interfacial charge polarization and multilevel structure interfacial scattering. Also, in common magnetic particles, nickel

and cobalt are toxic, and their applications are severely restricted in the fields of life science and medicines [13–15]. Iron oxide (Fe_3O_4, γ-Fe_2O_3) is usually used as a magnetic component, because of its low toxicity (LD_{50} about 2000 mg/kg, much higher than the current clinical application dose), availability, and so on [16–18].

The conductive polymers can be classified into the doping-type or intrinsic electroactive polymers. At present, poly-p-phenylene (PPP), polypyrrole (PPY), polythiophene (PTH), polyphenylacetylene (PPV), and polyaniline (PANI), with enormous monomers, have mostly been studied [19–22]. Compared with other conductive polymers, PANI attracts much more attentions of researchers due to its simple preparation method, excellent conductivity, and stability [23, 24]. In order to increase the multifunctional properties and get improved performances, many scientists have conducted extensive research on conductive polymer/magnetic particle composites, which possess advantages of both the magnetic and the conductive materials [25, 26].

Although previous researchers have prepared Fe_3O_4/-PANI nanocomposite, i.e., direct dispersion of magnetite nanoparticles in PANI solution or in situ preparation by polymerization of aniline in magnetite suspension [27–30], it is difficult to uniformly disperse the Fe_3O_4 nanoparticles in the PANI solution or prevent the oxidization of Fe_3O_4 nanoparticles by an oxidant (e.g., APS). In addition, the magnetic properties of Fe_3O_4/PANI nanocomposite are closely related to the size of the Fe_3O_4 particles. In order to synthesize uniformly dispersed Fe_3O_4 nanoparticles with smaller particle size and solve the drawbacks of the traditional in situ preparation method [31–35], the reverse in situ polymerization method was proposed, which alleviated the agglomeration of magnetic nanoparticles and inhibited the oxidation of magnetite. The magnetic properties and electrical conductivity of composite materials were investigated [36, 37].

2. Experimental

2.1. Materials. Aniline (AN), ferric chloride ($FeCl_3{\cdot}6H_2O$), ferrous sulfate ($FeSO_4{\cdot}7H_2O$), ammonium persulfate ($(NH_4)_2S_2O_8$), ammonia water (25%), ammonium persulfate, and chloroform were of analytical grade and used as received. 4-Dodecylbenzenesulfonic acid (DBSA, 96%) and 1 M hydrochloric acid were used directly. All the aqueous solutions were deionized water used as a solvent.

2.2. Preparation of PANI Chloroform Solution. 100 mL of deionized water was added to a three-necked flask; 1.40 g of AN and 1.46 g of DBSA were added in turn with vigorous agitation. Then, 0.56 g of additional AN was added to the flask, and the solution became milky white. After the suspension was kept at a constant temperature of 5°C by the ice water bath, 50 mL of ammonium persulfate aqueous solution (68.4 g/L) was added dropwise. The reaction mixture was stirred continuously, and the color change was observed. A complete reaction has taken place until the color changed from milky white to yellowish green, blue, blue-green, green, and dark green. Finally, extraction with 300 mL of chloroform was performed to obtain the PANI chloroform solution.

2.3. Preparation of PANI/Fe_3O_4 Nanocomposite. 30 mL of PANI chloroform solution was poured into a three-necked flask. 70 mL of $FeCl_3{\cdot}6H_2O$ aqueous solution (0.1 mol/L) and 40 mL of $FeSO_4{\cdot}7H_2O$ aqueous solution (0.1 mol/L) were added to the chloroform solution in sequence and stirred continuously to form an emulsion in nitrogen atmosphere. 10 mL ammonia water was then quickly added to the mixture when the temperature rose to 60°C. After stirring for 1 hour at 80°C, the flask was cooled down to room temperature. At last, extraction with 300 mL of chloroform was carried out to obtain the suspension containing PANI/Fe_3O_4 nanocomposite. The suspension would be washed using the deionized water for five times.

2.4. Characterization. The analysis of the surface functional groups of magnetic nanoparticles was done using the Acotar 360 type Fourier transform infrared (FT-IR) spectrometer. The particle size and crystalline structure of the nanocomposite were observed using a Hitachi H-600 transmission electron microscope (TEM) and an X-ray powder diffractometer (XRD, Japanese Society of Science and Technology D/Max-IIIC). The magnetic properties of nanocomposite were studied by a Gouy magnetic balance and a vibrating sample magnetometer. The electrical conductivity of Fe_3O_4/PANI chloroform solution was measured using a conductivity meter (DDS-11C, Leici Instruments Co. Ltd., Shanghai, China). Dielectric constant and magnetic permeability of nanocomposite at 2~18 GHz were measured using an Agilent 8720E vector network analyzer. The pure Fe_3O_4 nanoparticles were made similarly using coprecipitation. All the tests performed in this work were repeated for at least three times.

3. Results and Discussion

3.1. Composition Analysis. Figure 1 shows the FI-IR spectra of pure Fe_3O_4 nanoparticles and Fe_3O_4/PANI nanocomposite. The absorption peaks at 560.34 cm^{-1} and 577.30 cm^{-1} in both curves are the characteristic absorption peaks of Fe-O bonds. The peak at 3419.6 cm^{-1} in Figure 1(a) is a strong absorption peak of hydroxyl groups [38, 39]. This indicates that the surface of Fe_3O_4 magnetic nanoparticles is rich in hydroxyl groups, which is the basis for the surface modification of nanoparticles. The absorption peaks at 1491.56 cm^{-1} and 1299.61 cm^{-1} in Figure 1(b) correspond to the C=C stretching vibration of the quinone ring and C-N stretching vibration, respectively. 1124.62 cm^{-1} is the vibration absorption peak of quinone nitrogen atom, which indicates that PANI has been successfully coated onto the surface of Fe_3O_4 particles [40–43].

3.2. Structural Characterization. Figure 2(a) is the XRD pattern of Fe_3O_4 nanoparticles. As it can be seen, the characteristic peaks were at 30.03° (220), 35.41° (311), 43.0° (400), 53.0° (422), 57.0° (511), 62.6° (440), and 74.6° (533) as compared with the JCPDS standard card (No. 75-1609). This indicates that the obtained Fe_3O_4 particles are inverse-spinel type. According to the Scherrer formula $D = K\lambda/(\beta \cos\theta)$ (K is the Scherrer constant,

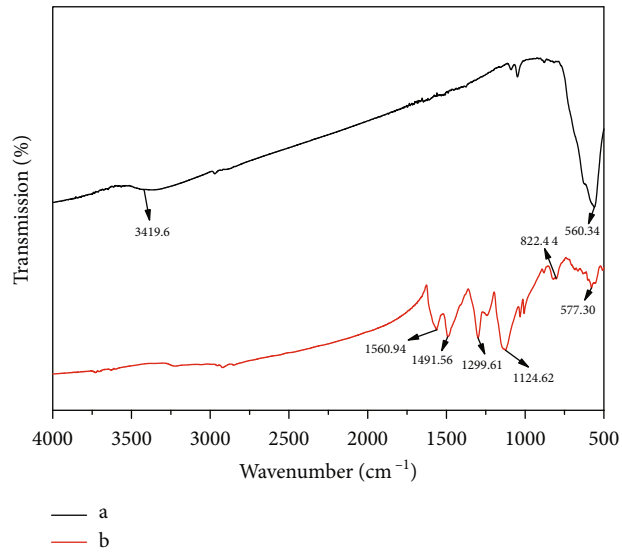

Figure 1: FT-IR spectra of (a) pure Fe_3O_4 nanoparticles and (b) Fe_3O_4/PANI nanocomposite.

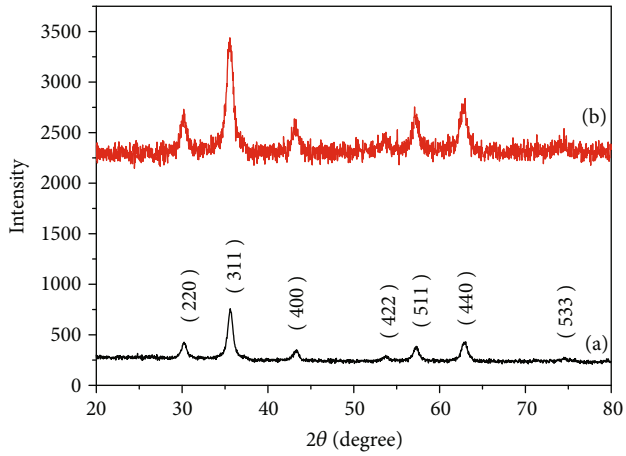

Figure 2: XRD spectra of (a) pure Fe3O4 nanoparticles and (b) Fe3O4/PANI nanocomposite.

λ is the X-ray wavelength, θ is the Bragg diffraction angle, and β is the half-peak width of the diffraction peak), the average particle size of the particles is calculated to be 10 nm.

Figure 2(b) is the XRD pattern of Fe_3O_4/PANI nanocomposite. It can be seen that new diffraction peak appears at 20°~30° due to the parallel vertical periodicity of the PANI chain, indicating that PANI has been successfully integrated with Fe_3O_4 [44, 45]. In addition, after integration with PANI, the characteristic peak of Fe_3O_4 remains, and just the intensity and width of the peak are changed, indicating that the particle is still the inverse-spinel type. It is worthwhile to note that the coating does not change the crystalline structure of the nanoparticles.

3.3. Morphology Characterization. Figure 3(a) is a TEM image of PANI, from which it can be seen that PANI is a fiber-interwoven network structure. Figure 3(b) shows that the Fe_3O_4 nanoparticles with a particle size of about 10 nm are uniformly embedded in the network structure of PANI. The Fe_3O_4 nanoparticles prepared through reverse in situ polymerization are smaller than those in the in situ polymerization. This may be related to the PANI formation [37, 40]. The scattered PANI acts as a coating agent and a surfactant, which inhibits the growth of Fe_3O_4 nanoparticles to preferentially avoid the agglomeration of Fe_3O_4 nanoparticles.

3.4. Magnetic Property Analysis. Figure 4 shows the hysteresis loops of pure Fe_3O_4 nanoparticles and Fe_3O_4/PANI nanocomposite. It can be perceived that both materials are superparamagnetic. The saturation magnetization of pure Fe_3O_4 nanoparticles was 84.83 emu/g. After the combination of Fe_3O_4 with PANI, the saturation magnetization of the nanocomposite decreased significantly, which was about 70.12 emu/g. This was mainly because the nonmagnetic PANI coated on Fe_3O_4 nanoparticles, resulting in a decrease in the relative content of Fe_3O_4 in the Fe_3O_4/PANI nanocomposite, so the saturation magnetization per unit mass was inevitably reduced [38, 42, 44, 46].

Figure 5 shows the relationship between the magnetic weight of the Fe_3O_4/PANI chloroform suspension and the applied magnetic field intensity. The magnetic weight of the Fe_3O_4/PANI chloroform suspension has a good linear relationship with the applied magnetic field intensity under a relatively low intensity of magnetic field (less than 30 mT). According to the slope of the magnetic weight and the applied magnetic field intensity curve, the magnetic susceptibility of the Fe_3O_4/PANI chloroform suspension was calculated as about 7.51×10^{-5}.

3.5. Conductivity Analysis of Chloroform Suspension. In the present work, the conductivity of chloroform suspension containing PANI and magnetic nanoparticles was determined. As listed in Table 1, the chloroform and chloroform-AN monomer solutions are not conductive. With the addition of surfactant DBSA, the solution begins to be electrically conductive with a conductivity of about 0.145 μS/cm, which can be attributed to the free movement of the anions and cations of the surfactant. After the polymerization of the AN monomer, the conductivity of the PANI chloroform solution was significantly improved and increased to 1.172 μS/cm. This is due to the presence of large conjugated groups in the PANI structure [41, 47–50], whereby the free movement of electrons is improved.

When Fe_3O_4 nanoparticles were formed in situ in PANI chloroform solution, the conductivity of the suspension was further increased to 1.835 μS/cm. This may be due to the fact that the Fe_3O_4 is an ionic crystal with more free electrons and hence increasing the density of the electron cloud. A similar experimental phenomenon was reported by Husain et al. [51]. When the amount of AN monomer is increased, the conductivity of the PANI chloroform solution containing magnetic nanoparticles continues to increase to a climax of 1.923 μS/cm, which is clearly attributed to the increase in PANI concentration in the suspension. At the same time, it can be seen that the solution conductivity increases as the amount of DBSA is increased. The PANI molecule exists in

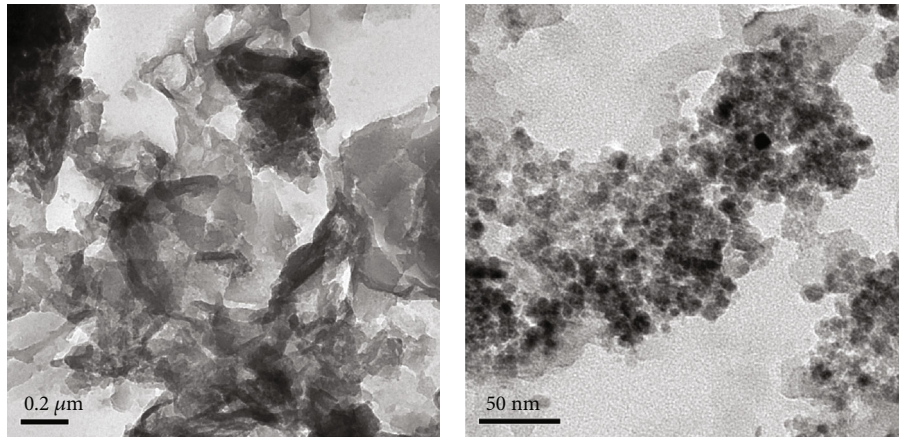

Figure 3: TEM images of (a) PANI and (b) Fe_3O_4/PANI nanocomposite.

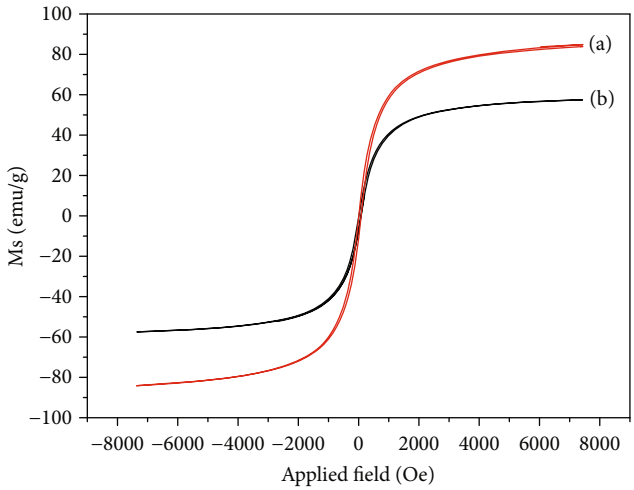

Figure 4: Magnetization curves of (a) pure Fe_3O_4 and (b) Fe_3O_4/PANI nanocomposite.

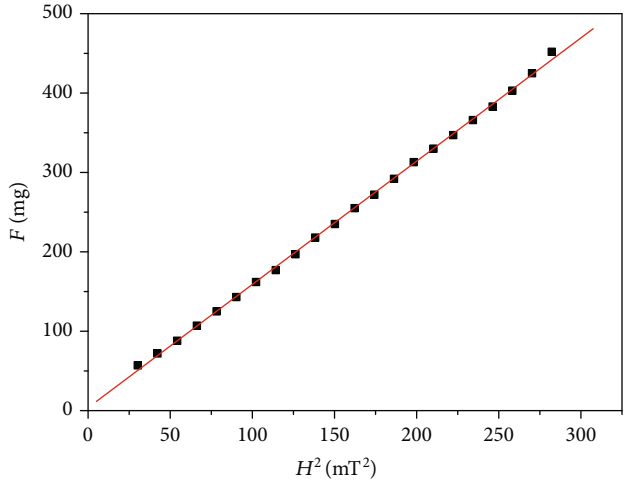

Figure 5: Relationship of magnetic weight and magnetic field intensity.

Table 1: Electrical conductivity of the samples.

Materials	Electrical conductivity (μS/cm)
$CHCl_3$	0
AN (1.96 g)+$CHCl_3$	0
AN (1.96 g)+DBSA (1.46 g)+$CHCl_3$	0.145
PANI (1.96 g AN)+DBSA (1.46 g)+$CHCl_3$	1.172
PANI (1.96 g AN)+DBSA (1.46 g)+Fe_3O_4+$CHCl_3$	1.835
PANI (2.66 g AN)+DBSA (1.46 g)+Fe_3O_4+$CHCl_3$	1.923
PANI (2.66 g AN)+DBSA (1.56 g)+Fe_3O_4+$CHCl_3$	2.135

the conformation of the extended chain because of more DBSA, which is beneficial to the delocalization and transition of the charge, resulting in higher conductivity.

From the abovementioned, we can conclude that the main factors affecting the conductivity of PANI chloroform suspension are the concentration of PANI, the amount of DBSA, and magnetic nanoparticles.

3.6. Electromagnetic Parameter Analysis. The suspension containing PANI/Fe_3O_4 nanocomposite was washed with a large amount of deionized water to remove the DBSA and $(NH_4)_2SO_4$, then washed with acetone several times and followed by vacuum drying to obtain the Fe_3O_4/PANI nanocomposite powder sample. The nanocomposite and paraffin were mixed at a mass ratio of 1 : 1 to make a coaxial sample with an inner diameter of 3 mm and an outer diameter of 7 mm; then electromagnetic parameters were tested using an Agilent 8720E vector network analyzer.

The complex permittivity of Fe_3O_4 and Fe_3O_4/PANI is presented in Figure 6. The size of the real part of the dielectric constant is related to the amount of energy storage while the imaginary part is related to the electric field loss of the material [36, 52–56].

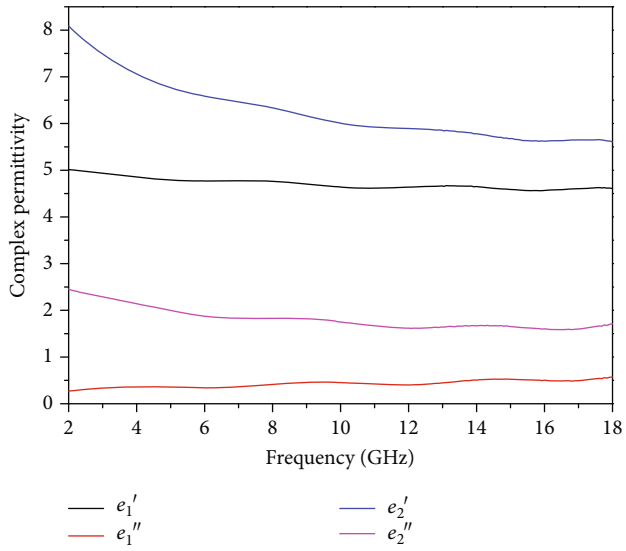

Figure 6: Complex permittivity curves of pure Fe_3O_4 (e_1) and Fe_3O_4/PANI nanocomposite (e_2).

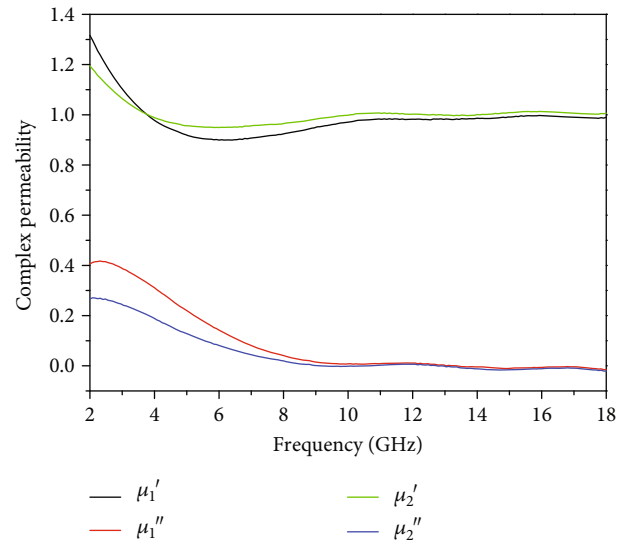

Figure 7: Complex permeability curves of pure Fe_3O_4 (μ_1) and Fe_3O_4/PANI nanocomposite (μ_2).

It is noticed that the real part ($e_2{}'$) and imaginary part ($e_2{}''$) of Fe_3O_4/PANI are higher than the respective part of Fe_3O_4 ($e_1{}'$, $e_1{}''$) in the range of 2~18 GHz. That is because PANI as a conductive polymer will produce many electric dipoles in the electric field, which will bind most of the energy of the electric field and eventually converted into heat. Meanwhile, the Fe_3O_4 is embedded in the PANI network structure which also increases the dielectric loss due to interfacial synergistic effects between the two materials [57–59].

The complex permeability of Fe_3O_4 and Fe_3O_4/PANI is presented in Figure 7. The real part (μ') is related to the amount of magnetic field energy storage while the imaginary part (μ'') is related to the magnetic field loss of the material.

The real part of the Fe_3O_4/PANI magnetic particles gradually decreases in the S-band (2~4 GHz). When the frequency is greater than 4 GHz, the real part slowly rises. This is because the Fe_3O_4 magnetic nanoparticles have a natural resonance in the S-band, and as the frequency increases, the "exchange mode resonance" between the magnetic nanoparticles becomes more and more obvious [60–62]. Also, the magnetic permeability of the S-band of Fe_3O_4 is relatively high, but as the frequency increases, the conjugated main chain structure of the conductive polymer inhibits the agglomeration of the magnetic nanoparticles, which reduce the reflection of electromagnetic waves and enhance the energy storage capacity of the composite material. Therefore, the real part of the Fe_3O_4/PANI nanocomposite is slowly increased at 4~18 GH_Z. The imaginary part of the Fe_3O_4/PANI nanocomposite is smaller than that of the pure Fe_3O_4 in the range of 2~18 GHz. This may be because the PANI encapsulates the magnetic nanoparticles to cause a decrease in saturation magnetization and a decrease in hysteresis loss [63, 64].

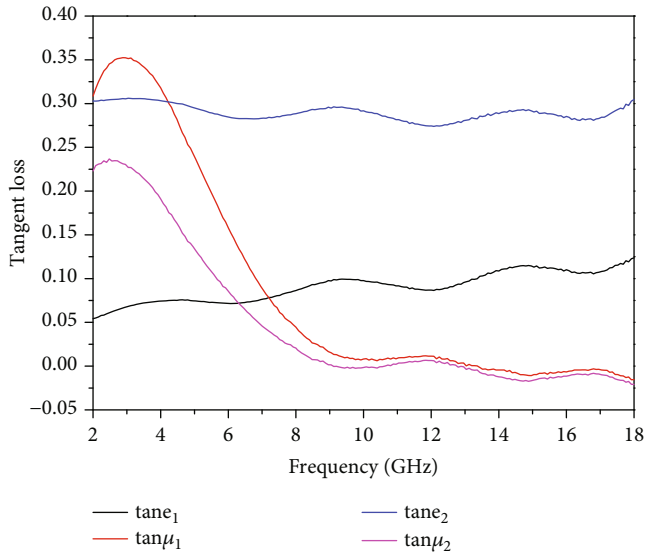

Figure 8: Tangent loss curves of pure Fe_3O_4 (e_1; μ_1) and Fe_3O_4/PANI nanocomposite (e_2; μ_2).

From Figure 8, the perception is made about the Fe_3O_4/PANI nanocomposite that the dielectric loss tangent is much larger than the magnetic loss tangent, which indicates that the effect of dielectric loss in 2~18 GHz is much larger than hysteresis loss. For pure Fe_3O_4 particles, dielectric loss is dominant with increasing frequency over 7.2 GHz. Figure 8 also displays that the magnetic loss tangent of the Fe_3O_4 particles is larger than that of the Fe_3O_4/PANI nanocomposite at 2~18 GHz [11, 65].

3.7. Refection Loss Curve Analysis. The electromagnetic wave properties of materials can be characterized by the RL,

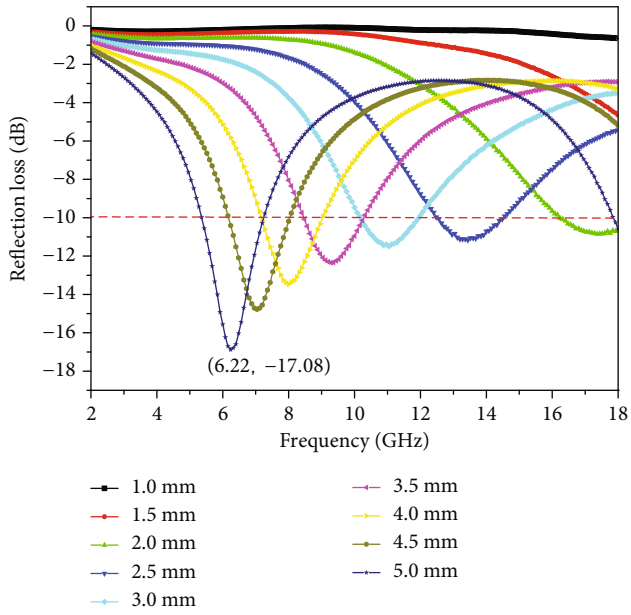

Figure 9: The calculated reflection losses curve of PANI/Fe_3O_4.

according to the transmission line theory. The RL can be expressed by the following equations:

$$\mathrm{RL} = -20 \log \frac{Z - Z_0}{Z + Z_0},$$
$$Z = \sqrt{\frac{\mu_r \mu_0}{e_r e_0}} \tanh \left[j \left(\frac{2\pi f d}{c} \right) \sqrt{\mu_r e_r} \right], \quad (1)$$

where Z_0 and Z are the impedance of free space and absorbing materials; μ_r and e_r are the complex permeability and complex dielectric constant of wave absorbing material; f is the frequency of the incident electromagnetic wave; d is the thickness of the absorber; and c is the velocity of light in free space [66–68].

The microwave reflectivity of Fe_3O_4/PANI nanocomposite is represented in Figure 9. PANI/Fe_3O_4 nanocomposite owns an excellent microwave absorbing property which includes a wide reflection (reflection loss < -10 dB) band (from 6.00 to 8.08 GHz) and has a minimum reflection value of -17.08 dB at 6.22 GHz at the thickness of 5.0 mm. Meanwhile, it is noticed that the thinner the coating, the more the absorbing band shifts towards low frequencies.

4. Conclusions

In this paper, the Fe_3O_4/PANI composite was successfully prepared by the reverse in situ polymerization method. The conductivity, magnetic properties, and microwave absorption properties of the composite were elaborated in detail. The conductivity of the suspension of PANI/Fe_3O_4 nanocomposite is higher than that of the pure PANI solution and increases with the increase of PANI concentration and DBSA. The dried PANI/Fe_3O_4 powder has a high saturation magnetization of 70.12 emu/g and owns an excellent microwave absorbing property, which includes a wide reflection (reflection loss < -10 dB) band (from 6.00 to 8.08 GHz) and has a minimum reflection value of -17.08 dB at 6.22 GHz at the thickness of 5.0 mm. The present work provides an evident basis for the preparation and potential applications of the electrical sensing and shielding coatings.

Data Availability

The data used to support the findings of this study are included within the article.

Conflicts of Interest

The authors declare that they have no conflicts of interest.

Authors' Contributions

Di Zhang, Huaiyin Chen, and Ruoyu Hong contributed equally to this work.

Acknowledgments

This research was financially supported by the National Natural Science Foundation of China (NSFC, No. 21246002), Minjiang Scholarship of Fujian Province (No. Min-Gao-jiao[2010]-117), Central Government-Guided Fund for Local Economic Development (No. 830170778), R&D Fund for Strategic Emerging Industry of Fujian Province (No. 82918001), International Cooperation Project of Fujian Science and Technology Department (No. 830170771), and Teaching and Researching Fund for Young Staff of Fujian Educational Department (No. JT180040).

References

[1] T. K. Gupta, B. P. Singh, R. B. Mathur, and S. R. Dhakate, "Multi-walled carbon nanotube-graphene-polyaniline multiphase nanocomposite with superior electromagnetic shielding effectiveness," *Nanoscale*, vol. 6, no. 2, pp. 842–851, 2014.

[2] D. X. Yan, H. Pang, B. Li et al., "Structured reduced graphene oxide/polymer composites for ultra-efficient electromagnetic interference shielding," *Advanced Functional Materials*, vol. 25, no. 4, pp. 559–566, 2015.

[3] Y. Chen, Y. L. Wang, H. B. Zhang, X. Li, C.-X. Gui, and Z.-Z. Yu, "Enhanced electromagnetic interference shielding efficiency of polystyrene/graphene composites with magnetic Fe_3O_4 nanoparticles," *Carbon*, vol. 82, pp. 67–76, 2015.

[4] B. Shen, Y. Li, W. Zhai, and W. Zheng, "Compressible graphene-coated polymer foams with ultralow density for adjustable electromagnetic interference (EMI) shielding," *ACS Applied Materials & Interfaces*, vol. 8, no. 12, pp. 8050–8057, 2016.

[5] P. Fedorko, J. Faurevincent, I. Fier et al., "Effect of structural anisotropy on electrical and magnetic properties of polyaniline conducting films," *Synthetic Metals*, vol. 166, no. 7, pp. 63–69, 2013.

[6] A. Ibrahim, M. H. Abdel-Aziz, M. S. Zoromba, and A. F. al-Hossainy, "Structural, optical, and electrical properties of multi-walled carbon nanotubes/polyaniline/Fe_3O_4 ternary nanocomposites thin film," *Synthetic Metals*, vol. 238, pp. 1–13, 2018.

[7] S. Shahabuddin, N. M. Sarih, S. Mohamad, and S. N. A. Baharin, "Synthesis and characterization of Co_3O_4 nanocube-doped polyaniline nanocomposites with enhanced methyl orange adsorption from aqueous solution," *RSC Advances*, vol. 6, no. 49, pp. 43388–43400, 2016.

[8] M. Novak, I. Kokanović, D. Babić, and M. Baćani, "Influence of disorder on electrical transport and magnetic properties of HCl- doped polyaniline pellets," *Journal of Non-Crystalline Solids*, vol. 356, no. 33-34, pp. 1725–1729, 2010.

[9] K. Yoshizawa, A. Ito, K. Tanaka, and T. Yamabe, "Magnetic property of soluble poly(*m*-aniline)," *Solid State Communications*, vol. 87, no. 10, pp. 935–937, 1993.

[10] M. Cernea, B. S. Vasile, V. A. Surdu et al., "Piezoelectric/ferromagnetic BNT- $BT_{0.08}/CoFe_2O_4$ coaxial core-shell composite nanotubes for nanoelectronic devices," *Journal of Alloys and Compounds*, vol. 752, pp. 381–388, 2018.

[11] Z. He, Y. Fang, X. Wang, and H. Pang, "Microwave absorption properties of PANI/CIP/Fe_3O_4 composites," *Synthetic Metals*, vol. 161, no. 5-6, pp. 420–425, 2011.

[12] Q. Gong, Y. Li, H. Huang, J. Zhang, T. Gao, and G. Zhou, "Shape-controlled synthesis of Ni-CeO_2@PANI nanocomposites and their synergetic effects on supercapacitors," *Chemical Engineering Journal*, vol. 344, pp. 290–298, 2018.

[13] R. A. Ana, S. Maryam, F. Marta et al., "Biochemical and behavioral responses of zebrafish embryos to magnetic graphene/nickel nanocomposites," *Ecotoxicology and Environmental Safety*, vol. 186, article 109760, 2019.

[14] D. Xu, L. Zhang, H. Wang, and Z. Bian, "Optimization of electrochemical sequential reduction-oxidation of chlorophene with CoNi alloy anchored ionic liquid-graphene cathode: comparison, mechanism and toxicity study," *Chemical Engineering Journal*, vol. 358, pp. 1371–1382, 2019.

[15] X. R. Wang and N. N. Song, "An improved biotic ligand model (BLM) for predicting Co(II)-toxicity to wheat root elongation: the influences of toxic metal speciation and accompanying ions," *Ecotoxicology and Environmental Safety*, vol. 182, pp. 109–113, 2019.

[16] Y. F. Yang, F. Y. Meng, X. H. Li et al., "Magnetic graphene oxide-Fe_3O_4-PANI nanoparticle adsorbed platinum drugs as drug delivery systems for cancer therapy," *Journal of Nanoscience and Nanotechnology*, vol. 19, no. 12, pp. 7517–7525, 2019.

[17] V. Madhubalaa, T. Kalaivania, A. Kirubha, J. S. Prakash, V. Manigandan, and H. K. Dara, "Study of structural and magnetic properties of hydro/solvothermally synthesized α-Fe_2O_3 nanoparticles and its toxicity assessment in zebrafish embryos," *Applied Surface Science*, vol. 15, pp. 391–400, 2019.

[18] J. Wu, J. Ding, P. Wang et al., "Cellular uptake, stability, and safety of hollow carbon sphere-protected Fe_3O_4 nanoparticles," *Journal of Nanoscience and Nanotechnology*, vol. 20, no. 4, pp. 2584–2591, 2020.

[19] J. Luo, P. Shen, W. Yao, C. Jiang, and J. Xu, "Synthesis, characterization, and microwave absorption properties of reduced graphene oxide/strontium ferrite/polyaniline nanocomposites," *Nanoscale Research Letters*, vol. 11, no. 1, p. 141, 2016.

[20] M. E. Vaschetto, A. P. Monkman, and M. Springborg, "First-principles studies of some conducting polymers: PPP, PPy, PPV, PPyV, and PANI," *Journal of Molecular Structure: THEOCHEM*, vol. 468, no. 3, pp. 181–191, 1999.

[21] C. X. Bian, X. C. Xu, W. Yu et al., "Study on conductive mechanism of composites-sulfonated polyphenylacetylene/multi-walled carbon nanotubes," *Acta Physico-Chimica Sinica*, vol. 22, no. 10, pp. 1185–1190, 2007.

[22] J. Ding, L. Wang, Y. Zhao et al., "Boosted interfacial polarization from multishell TiO_2@Fe_3O_4@PPy heterojunction for enhanced microwave absorption," *Small*, vol. 15, article 1902885, 2019.

[23] Y. Zhang, Y. Duan, L. Song, D. Zheng, M. Zhang, and G. Zhao, "Charge-transfer mobility and electrical conductivity of PANI as conjugated organic semiconductors," *The Journal of Chemical Physics*, vol. 147, no. 11, pp. 114–121, 2017.

[24] T. Hao, W. Wang, and D. Yu, "A flexible cotton-based supercapacitor electrode with high stability prepared by multiwalled CNTs/PANI," *Journal of Electronic Materials*, vol. 47, no. 7, pp. 4108–4115, 2018.

[25] I. J. Moon, M. W. Kim, H. J. Choi, N. Kim, and C.-Y. You, "Fabrication of dopamine grafted polyaniline/carbonyl iron core-shell typed microspheres and their magnetorheology," *Colloids and Surfaces A: Physicochemical and Engineering Aspects*, vol. 500, pp. 137–145, 2016.

[26] F. Movassagh-Alanag, A. Bordbar-Khiabani, and A. Ahangari-Asl, "Fabrication of a ternary PANI@Fe_3O_4@CFs nanocomposite as a high performance electrode for solid-state supercapacitors," *International Journal of Hydrogen Energy*, vol. 44, no. 49, pp. 26794–26806, 2019.

[27] M. R. Patil, S. D. Khairnar, and V. S. Shrivastava, "Synthesis, characterisation of polyaniline-Fe_3O_4 magnetic nanocomposite and its application for removal of an acid violet 19 dye," *Applied Nanoscience*, vol. 6, no. 4, pp. 495–502, 2016.

[28] A. Katunin, K. Krukiewicz, R. Turczyn, P. Sul, A. Łasica, and M. Bilewicz, "Synthesis and characterization of the electrically conductive polymeric composite for lightning strike protection of aircraft structures," *Composite Structures*, vol. 159, pp. 773–783, 2017.

[29] F. Chen, A. Chen, and Y. Zhao, "Morphology controllable fabrication and conductive magnetic properties of nano Fe_3O_4/polypyrrole composites," *Acta Materiae Compositae Sinica*, vol. 32, no. 4, pp. 955–961, 2015.

[30] X. Han, "Effect of emulsion polymerization conditions on the electromagnetic properties of magnetic and conductive polyaniline nanoparticles," *Journal of Functional Materials and Devices*, vol. 23, no. 4, pp. 98–101, 2007.

[31] R. Li, L. Liu, and F. Yang, "A study on the reduction behaviors of Cr(VI) on Fe_3O_4/PANI," *Procedia Environmental Sciences*, vol. 18, pp. 522–527, 2013.

[32] C. Jia, D. Lu, B. Wu et al., "Synthesis and electrochromic properties of conducting polymers: polyaniline directly grown on fluorine-doped tin oxide substrate via hydrothermal techniques," *Solar Energy Materials & Solar Cells*, vol. 177, pp. 70–74, 2017.

[33] R. Y. Hong, J. H. Li, H. Z. Li, J. Ding, Y. Zheng, and D. G. Wei, "Synthesis of Fe_3O_4 nanoparticles without inert gas protection used as precursors of magnetic fluids," *Journal of Magnetism and Magnetic Materials*, vol. 320, no. 9, pp. 1605–1614, 2008.

[34] R. Y. Hong, T. T. Pan, and H. Z. Li, "Microwave synthesis of magnetic Fe_3O_4 nanoparticles used as a precursor of nanocomposites and ferrofluids," *Journal of Magnetism and Magnetic Materials*, vol. 303, no. 1, pp. 60–68, 2006.

[35] T. Mahmoudi-Badiki, S. S. S. Afghahi, N. Arsalani, M. Jafarian, and C. A. Stergiou, "Effect of synthesis approaches and

morphological properties on dielectric enhancement and microwave absorption of Fe_3O_4/PANI nanocomposites," *Journal of Superconductivity and Novel Magnetism*, vol. 32, no. 6, pp. 1705–1714, 2019.

[36] X. Ding, D. Han, Z. Wang, X. Xu, L. Niu, and Q. Zhang, "Micelle-assisted synthesis of polyaniline/magnetite nanorods by in situ self-assembly process," *Journal of Colloid and Interface Science*, vol. 320, no. 1, pp. 341–345, 2008.

[37] G. Song, J. Han, and R. Guo, "Synthesis of polyaniline/NiO nanobelts by a self-assembly process," *Synthetic Metals*, vol. 157, no. 4-5, pp. 170–175, 2007.

[38] X. Sun, X. Lv, X. Li, X. Yuan, L. Li, and G. Gu, "Fe_3O_4@SiO_2 nanoparticles wrapped with polypyrrole (PPy) aerogel: a highly performance material as excellent electromagnetic absorber," *Materials Letters*, vol. 221, pp. 93–96, 2018.

[39] Z. Liu, S. Yang, Z. Li et al., "Three-layer core-shell magnetic Fe_3O_4@C@Fe_2O_3 microparticles as a high-performance sorbent for the capture of gaseous arsenic from SO_2-containing flue gas," *Chemical Engineering Journal*, vol. 378, article 122075, 2019.

[40] X. Yao, X. Kou, and J. Qiu, "Generation mechanism of negative dielectric properties of nano-Fe_3O_4/PANI composites," *Materials Chemistry and Physics*, vol. 208, pp. 177–182, 2018.

[41] L. Gai, X. Han, Y. Hou, J. Chen, H. Jiang, and X. Chen, "Surfactant-free synthesis of Fe_3O_4@PANI and Fe_3O_4@PPy microspheres as adsorbents for isolation of PCR-ready DNA," *Dalton Transactions*, vol. 42, no. 5, pp. 1820–1826, 2013.

[42] R. F. Bianchi, H. N. da Cunha, R. M. Faria, G. F. Leal Ferreira, and J. M. G. Neto, "Electrical studies on the doping dependence and electrode effect of metal–PANI–metal structures," *Journal of Physics D: Applied Physics*, vol. 38, no. 9, pp. 1437–1443, 2005.

[43] E. E. Tanriverdi, A. T. Uzumcu, H. Kavas, A. Demir, and A. Baykal, "Conductivity Study of Polyaniline-Cobalt Ferrite (PANI-$CoFe_2O_4$) Nanocomposite," *Nano-Micro Letters*, vol. 3, no. 2, pp. 99–107, 2011.

[44] P. Liu, Y. Huang, Y. Yang, J. Yan, and X. Zhang, "Sandwich structures of graphene@Fe_3O_4@PANI decorated with TiO_2 nanosheets for enhanced electromagnetic wave absorption properties," *Journal of Alloys and Compounds*, vol. 662, pp. 63–68, 2016.

[45] N. Dong, M. Zhong, P. Fei, Z. Lei, and B. Su, "Magnetic and electrochemical properties of PANI- $CoFe_2O_4$ nanocomposites synthesized via a novel one-step solvothermal method," *Journal of Alloys and Compounds*, vol. 660, pp. 382–386, 2016.

[46] M. Almasi-Kashi, M. H. Mokarian, and S. Alikhanzadeh-Arani, "Improvement of the microwave absorption properties in FeNi/PANI nanocomposites fabricated with different structures," *Journal of Alloys and Compounds*, vol. 742, pp. 413–420, 2018.

[47] S. Wu, F. Su, X. Dong et al., "Development of glucose biosensors based on plasma polymerization-assisted nanocomposites of polyaniline, tin oxide, and three-dimensional reduced graphene oxide," *Applied Surface Science*, vol. 401, pp. 262–270, 2017.

[48] X. Zhu, J. Niu, F. Zhang, J. Zhou, X. Li, and J. Ma, "Preparation of recoverable Fe_3O_4@PANI–Pd^{II} core/shell catalysts for Suzuki carbonylative cross-coupling reactions," *New Journal of Chemistry*, vol. 38, no. 9, pp. 4622–4627, 2014.

[49] A. A. Jatratkar, J. B. Yadav, R. R. Deshmukh, H. C. Barshilia, V. Puri, and R. K. Puri, "Impact of low-pressure glow-discharge-pulsed plasma polymerization on properties of polyaniline thin films," *Physica Scripta*, vol. 91, no. 12, article 125501, 2016.

[50] J. Deng, X. Ding, W. Zhang et al., "Magnetic and conducting Fe_3O_4 –cross-linked polyaniline nanoparticles with core–shell structure," *Polymer*, vol. 43, no. 8, pp. 2179–2184, 2002.

[51] J. Husain, P. Pradeep, N. Raghu et al., "Synthesis, conductivity and sensitivity studies of polyaniline -iron oxide nanocomposites," *Ferroelectrics*, vol. 505, no. 1, pp. 229–235, 2016.

[52] S. P. Pawar, G. Melo, and U. Sundararaj, "Dual functionality of hierarchical hybrid networks of multiwall carbon nanotubes anchored magnetite particles in soft polymer nanocomposites: Simultaneous enhancement in charge storage and microwave absorption," *Composites Science and Technology*, vol. 183, p. 107802, 2019.

[53] L. Pan, B. C. Park, M. Ledwig, L. Abelmann, and Y. K. Kim, "Magnetic particle spectrometry of Fe_3O_4 multi-granule nanoclusters," *IEEE Transactions on Magnetics*, vol. 53, no. 11, pp. 1–5, 2017.

[54] A. S. Bongiovanni, E. I. Yslas, C. R. Rivarola, and C. A. Barbero, "Synthesis of polyaniline (PANI) and functionalized polyaniline (F-PANI) nanoparticles with controlled size by solvent displacement method. Application in fluorescence detection and bacteria killing by photothermal effect," *Nanotechnology*, vol. 29, no. 12, article 125604, 2018.

[55] M. I. M. Yazid, S. A. Ghani, A. F. Osman, S. H. M. Din, and T. S. Jin, "The effect on poly (ethylene oxide) / poly (vinyl chloride) / polyaniline (PANI) films by ethylene dimethacrylate as surface modifier: electrical conductivity and characterization," *Journal of Physics Conference Series*, vol. 908, article 012007, 2017.

[56] Y. Zou, Z. Zhang, W. Zhong, and W. Yang, "Hydrothermal direct synthesis of polyaniline, graphene/polyaniline and N-doped graphene/polyaniline hydrogels for high performance flexible supercapacitors," *Journal of Materials Chemistry A*, vol. 6, no. 19, pp. 9245–9256, 2018.

[57] M. Qiu, Z. Yang, and B. Wen, "Facile synthesis of polyaniline nanostructures with effective electromagnetic interference shielding performance," *Journal of Materials Science Materials in Electronics*, vol. 29, no. 12, pp. 10437–10444, 2018.

[58] C. Zhu, F. Liu, L. Song, H. Jiang, and A. Li, "Magnetic Fe_3O_4@-polyaniline nanocomposites with a tunable core-shell structure for ultrafast microwave-energy-driven reduction of Cr(VI)," *Environmental Science: Nano*, vol. 5, no. 2, pp. 487–496, 2017.

[59] S. Zeghina, J. Wojkiewicz, S. Lamouri, B. Belaabed, and N. Redon, "Enhanced microwave absorbing properties of lightweight films based on polyaniline/aliphatic polyurethane composites in X band," *Journal of Applied Polymer Science*, vol. 131, no. 21, article 40961, 2015.

[60] Y. Xu, J. Luo, W. Yao, J. Xu, and T. Li, "Preparation of reduced graphene oxide/flake carbonyl iron powders/polyaniline composites and their enhanced microwave absorption properties," *Journal of Alloys and Compounds*, vol. 636, pp. 310–316, 2015.

[61] C. Ding, Y. Zhu, M. Liu, L. Feng, M. Wan, and L. Jiang, "PANI nanowire film with underwater superoleophobicity and potential-modulated tunable adhesion for no loss oil droplet transport," *Soft Matter*, vol. 8, no. 35, pp. 9064–9068, 2012.

[62] K. Gheisari, S. Javadpour, H. Shokrollahi, and B. Hashemi, "Magnetic losses of the soft magnetic composites consisting of iron and Ni-Zn ferrite," *Journal of Magnetism and Magnetic Materials*, vol. 320, no. 8, pp. 1544–1548, 2008.

[63] L. J. Wu, Z. Q. Zhu, D. Staton, M. Popescu, and D. Hawkins, "Analytical modeling and analysis of open-circuit magnet loss in surface-mounted permanent-magnet machines," *IEEE Transactions on Magnetics*, vol. 48, no. 3, pp. 1234–1247, 2012.

[64] M. Desvaux, S. Sire, S. Hlioui, H. Ben Ahmed, and B. Multon, "Development of a hybrid analytical model for a fast computation of magnetic losses and optimization of coaxial magnetic gears," *IEEE Transactions on Energy Conversion*, vol. 34, no. 1, pp. 25–35, 2019.

[65] X. Weng, X. Lv, B. Li et al., "One-pot preparation of reduced graphene oxide/carbonyl iron/polyvinyl pyrrolidone ternary nanocomposite and its synergistic microwave absorbing properties," *Materials Letters*, vol. 188, pp. 280–283, 2017.

[66] B. Zhang, Y. Du, P. Zhang et al., "Microwave absorption enhancement of Fe_3O_4/polyaniline core/shell hybrid microspheres with controlled shell thickness," *Journal of Applied Polymer Science*, vol. 130, no. 3, pp. 1909–1916, 2013.

[67] B. Zhang, C. Lu, and L. Hai, "Improving microwave adsorption property of ZnO particle by doping graphene," *Materials Letters*, vol. 116, no. 2, pp. 16–19, 2014.

[68] M. Jafarian, S. S. S. Afghahi, Y. Atassi, and M. Salehi, "Enhanced microwave absorption characteristics of nanocomposite based on hollow carbonyl iron microspheres and polyaniline decorated with MWCNTs," *Journal of Magnetism and Magnetic Materials*, vol. 462, pp. 153–159, 2018.